17th World Conference on Earthquake Engineering, 17WCEE
Sendai, Japan - September 13th to 18th 2020

SPATIAL CORRELATION OF LOSSES IN JAPAN: IMPACT OF EARTHQUAKE AND TSUNAMI SOURCE MODEL ASSUMPTIONS

D.D. Fitzenz(1), S. Levy(1), L. Damiao(1), R. Jalali Farahani(1), J. Woessner(2)

(1) Earthquake Model Development, Risk Management Solutions, Inc., Newark, CA, USA, *Delphine.Fitzenz@rms.com*, *Sam.Levy@rms.com*, *Landon.Damiao@rms.com*, *Rozita.Farahani@rms.com*,
(2) Earthquake Model Development, Risk Management Solutions, Inc., Zurich, 8050, Switzerland, *Jochen.Woessner@rms.com*

Abstract

Post Tohoku, most countries have strived to ensure that they include the largest events that cannot be ruled out, as opposed to the largest event that has been observed plus some uncertainty. This included considering not only M9s on the Japan Trench, but also M9 on the Nankai trench, as well as a larger seismogenic area offshore Tokyo (Sagami trough, Chokkagata sources) (ERC, 2016) and more recently M9 on the Kuril trench (ERC 2018). Outside of Japan, M9s are considered for New Zealand (Hikurangi subduction) and Indonesia. Even for non-subduction countries, this "all that cannot be ruled out" perspective has led to the inclusion of very large multi-fault events (California). When such events are introduced, they change both the site-source distance and the partitioning of the seismic budget. Their geometrical aspects, which affect hazard and damage footprints, and the modelling of their recurrence impact the risk landscape of a country. For California, Fitzenz et al. 2018 [1] looked at the impact of both segmentation assumptions and time-dependent modelling assumptions on the spatial correlations of expected losses in Bay Area and southern California counties. Quantifying and understanding spatial correlation changes of expected loss has important implications for a robust assessment of the level of diversification in an existing portfolio of risk as well as for the implementation or updating of underwriting guidelines.

When most of the large events newly introduced into a model can also cause tsunami losses, the question becomes more layered. What are the spatial correlations across coastal city wards in Japan? How do they change depending on the recurrence modelling perspective? What correlations come from shake losses-only versus tsunami losses? We present results obtained using the RMS High Definition Japan Earthquake and Tsunami model. The sophisticated treatment of source characteristics and wave dynamics as well as the high resolution of the model allows us to highlight the far-reaching (and not necessarily intuitive) impact of tsunami events. This helps establish in which contexts information on shake loss spatial correlation is a good guide for tsunami loss correlation. We also use the newly developed renewal model for Nankai (Fitzenz 2018 [2]) to explore how time-dependent modeling impacts the correlations. We choose a subset of coastal city wards with high insured exposed value to quantify those effects.

Such studies can help develop risk-based research priorities by pointing to where the need is the greatest to refine the physical characterization of the sources (lateral extent, up-dip and down-dip extent), recurrence model assumptions, slip distribution modelling, as well as bathymetry topography parameterization constraints that influence sea floor and coast deformation models. The outputs of this study can be valuable for the multi-hazard loss estimation of shaking and tsunami.

Keywords: risk; spatial correlations; earthquake source modelling; tsunami

1. Introduction

The M9 Tohoku event in 2011 reminded the world that megathrust earthquakes and tsunami not experienced in hundreds of years could happen and cause a lot of loss and destruction. For that reason, Japan and other countries have revised their hazard models and incorporated more very large events. For Japan, those include not only M9 Japan trench events like Tohoku, but also several possibilities for M>9 on the Nankai trough, M>8.5 on Sagami (ERC 2016 [3]) and M>9 on the Kuril trench (2018 update). Of course, those are not the only events that can cause tsunami: events M7.5 and larger can already occasionally cause waves and inundation damage. RMS implemented an earthquake and tsunami risk model for Japan based on the ERC

(2016) source model, with details described in a companion paper at this conference (Masuda et al, 2020 [4]).

The most common metrics used to assess catastrophe risk to an insured portfolio are average annual loss (AAL), annual exceedance probability (AEP), and occurrence exceedance probability (OEP). The former gives an overall perspective on the expected losses from a peril and can guide premium setting. The latter two are effective at describing the high-level losses to a region, crucial to define reserves and risk transfer strategies. However, these metrics fall short of describing the spatiotemporal relationship of losses between different regions. It is important for portfolio management to understand the exposure diversification of a portfolio. Two regions that have similar modeled average annual losses or return period losses can be great to do business in, as long as the loss causing events are not in common between the two regions. In that spirit, Fitzenz et al (2018 [1]) showed how risk selection in California can be affected by earthquake source modeling assumptions. In particular, the possibility for large events to go through fault segment boundaries and continue on to nearby faults or segments, can correlate various Southern California counties, and even the San Francisco Bay Area and the Greater Los Angeles area, a big contrast to previous perception in the industry.

Here we examine the spatial correlation of annual losses in Japan through the computation of the loss correlation between coastal city wards as defined in the Japan Earthquake Industry Exposure Database of RMS (2018). This is a model of the total insured value in each city ward. We use the RMS High Definition Japan Earthquake and Tsunami model to compute the losses. This model contains inventory assumptions and the corresponding vulnerability functions. We compare spatial correlations stemming from shake-only losses to spatial correlations related to tsunami losses. Since the practice of estimating tsunami risk by using shake losses with a factor is sometimes used, we find this comparison provides insight that could prevent misguided inferences on portfolio diversification. Though a similar exercise can be performed selecting only the events that contribute to long/short return period losses, we demonstrate the method and results using the full annual expected loss.

To this end, the first section of the paper presents the methods for tsunami and shake modeling as applied in the RMS HD Japan Earthquake and Tsunami model, as well as the method used to compute loss correlations. The results section shows loss and loss normalized by exposure value in coastal city wards, as well as expected loss correlation between coastal city wards.

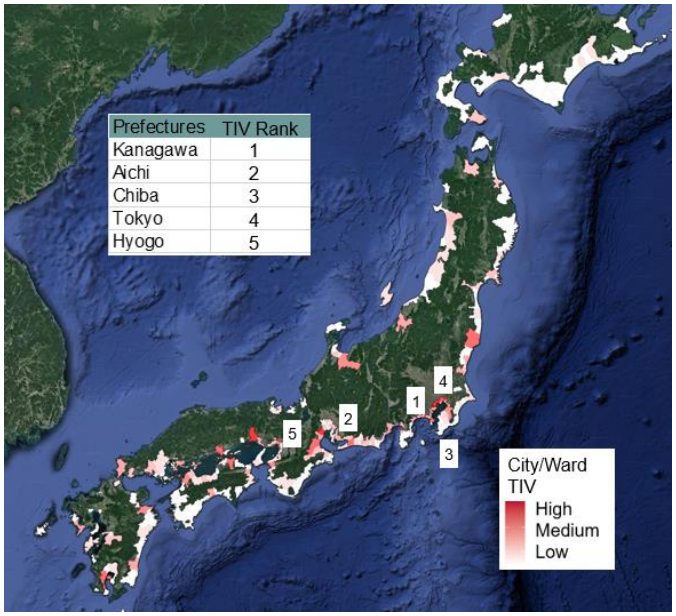

Fig. 1 – Map of Japan showing the CWs that include TS losses. The CWs are colored by TIV.

2. Methods

2.1 Tsunami and Shake Modeling

This section covers an overview of our high-definition probabilistic tsunami and shake models. Probabilistic Tsunami Hazard Assessment (PTHA) combines, similar to Probabilistic Seismic Hazard Assessment (PSHA), a set of individual components that are essential to estimate exceedance probabilities of an intensity parameter within a given time frame, such as exceedance probabilities of tsunami runup heights or maximum inundation levels within a given period. There are five major components to generate a PTHA:

1. Prepare an earthquake source model that defines the fault geometries, the magnitudes, and the annual rate of occurrence of the events;
2. Prepare an earthquake rupture model that defines how, for a given fault geometry and magnitude the slip is distributed across the fault plane;
3. Calculate the (elastic) dislocation in the study area and in particular across the rupture area as input for the initial tsunami wave calculation
4. Model the tsunami wave propagation across the sea, tsunami runup and inundation on the coast.
5. Combine the inundation results with the exposure, vulnerability, and financial model to estimate financial losses.

Each of these components has its range of possible solutions, in particular, the definition of earthquake sources is non-unique and needs to be treated in a probabilistic sense. Details of the RMS probabilistic tsunami models are given in an accompanying paper by Farahani et al. (2020, [5]) and Woessner & Farahani (2020, [6]). Earthquake ruptures on the subduction interface and faults in the oceanic crust can cause significant vertical and lateral displacement of the ocean floor generating a tsunami. Most ruptures are located on the primary interface, however, the rupture can potentially continue/ on splay faults in the accretion wedge. In general, thrust events are generating tsunamis, however, normal faulting events in the outer rise of the subduction plate can also cause tsunamis which is why the latter are included in this model.

The geometry and magnitudes of the tsunami sources are derived from the set of sources (Fig. 2) that are provided by HERP through the Japan Seismic Hazard Information Station (http://www.j-shis.bosai.go.jp/en/). Thereafter, multiple finite fault slip models using Melgar et al. (2016, [7]) are generated. While all these models are mathematically viable solutions, not all of those models are either physically possible neither are all prone to generate tsunami. The method primarily preserves the stochastic properties of the distribution of slip patches, while it does not consider physical constraints. The stochastic properties constrain the ratio of patches with small slip values to patches with large slip values and their spatial correlation.

It is therefore necessary to define a set of criteria to ensure that the ruptures generate a tsunami. Given the assumption that only events with $M_W \geq 7.5$ generate tsunamis considered to be significant also in terms of losses as well as the number of sources defined by the 2017 National seismic hazard map, more than 750 tsunamis are considered for tsunami risk in the RMS model.

Hydrodynamic characteristics of tsunami waves are influenced by the initial tsunami waveforms as well as the surrounding bathymetric and topographic profiles. To accurately model the variations of tsunami height and length during wave propagation and coastal inundation, we solve the nonlinear shallow water equations using finite volume numerical method. To accelerate the comprehensive computational efforts, parallel computation on Graphic Processing Units (GPUs) was implemented. Three levels of nested grids with different resolutions are used to perform the numerical modeling and capture the coastal processes including wave reflection, diffraction, and refraction. The finest grids have a resolution of 50 m_2 covering the eastern and western Japan coastlines. The numerical model is run for 6 hours after the generation of the tsunami waves to model the full lifetime of tsunami waves, coastal processes, and coastal inundation.

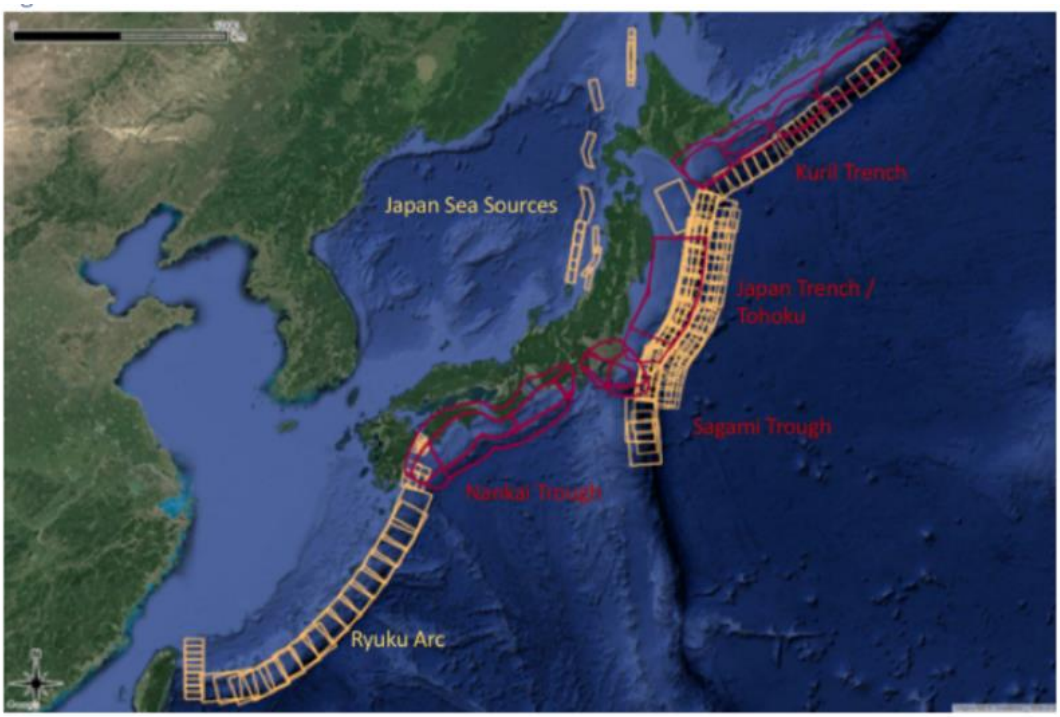

Fig. 2 – Location of tsunamigenic sources for the RMS Japan PTHA model. Large interface sources (red) are differentiated from the smaller interface/intraplate, outer rise and Japan sea sources (yellow).

The tsunami modeling approach is illustrated for an M9 type earthquake on the Tohoku source as defined by [3] (Fig. 3). The non-uniform slip distributions display possible scenarios with two high-slip concentrations (Fig. 3a). Deformation just on top of the rupture plane reaches slightly more than 12m, generating the initial water column uplift of about the same level (Fig. 3b). Subsidence along the coast reach peak values above 5m which is larger than what has been observed in the GPS-observations of the 2011 Tohoku event. It needs to be noted that the purely elastic deformation may overestimate the actual measured deformation values as crustal deformation is not limited to elastic deformation and thus deformation tends to be smaller in reality. Inundation results for this example is displayed for the Sendai plane with maximum inundation values up to 20m (Fig. 3a).

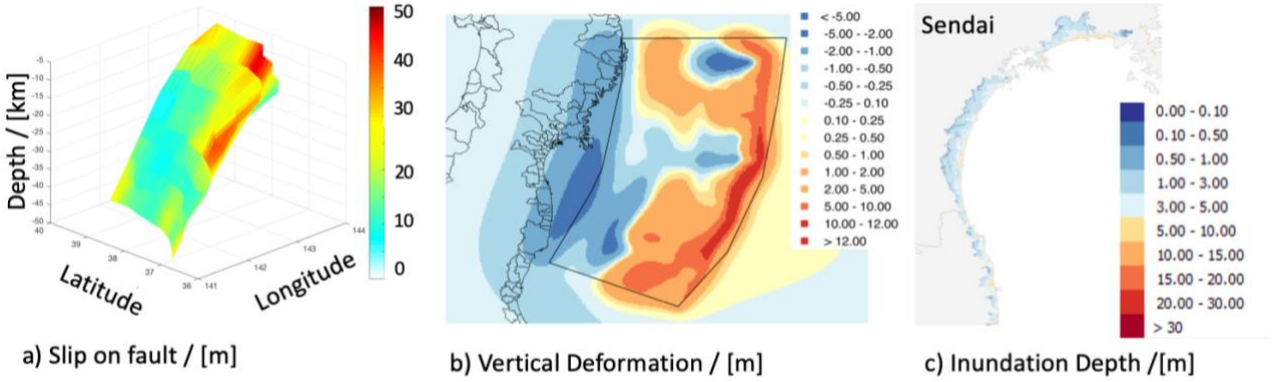

Fig. 3 – Example results of the tsunami modeling steps for a Tohoku Mw9 type earthquake. a) Simulated distributed slip on the fault plane, b) Vertical elastic deformation (subsidence / uplift), and c) Inundation depth along the coast of the Sendai plane.

RMS Japan probabilistic shake model includes different components as below:

(1) Source Modelling: Our model is based on the ERC [3] database of earthquake sources. Several original improvements have been applied to the mean recurrence time [2,4]
(2) Ground Motion: Ground motion prediction equations (GMPEs) predict the mean ground shaking level at a site as a function of various factors, which include source, path (i.e. site-to-source distance) and site effects along with the ground motion uncertainty. The details of our ground motion model are discussed in Kwak & Seyhan, 2020 [8]. This is in contrast to the wave simulation methodology used for the tsunami modeling.
(3) Geotechnical characteristics: Geotechnical data are an important input for site amplification models that modify the ground shaking by incorporating the local site conditions. More details can be found in Masuda et al, 2020 [4].
(4) Vulnerability Assessment: We developed vulnerability functions based on the latest research studies in performance-based earthquake engineering. The details of our vulnerability model are discussed in [4].

2.2 Loss Correlation Method and Implementation:

While this paper is mostly focused on those shake events that also cause tsunami, the RMS HD Japan Earthquake and Tsunami model is a full representation of potentially loss causing seismic sources in Japan. Those include known crustal fault events, megathrust interface events, outer rise events, but also a host of potential events whose rate and location and magnitude are derived from catalog analysis: crustal background events as well as interface and intraslab background, minor and medium events. The range in event rates is between less than 10^{-8} to higher than 10^{-2} per year, with most events ranging between 10^{-6} and 10^{-3} per year. The reference view for risk in the RMS product is time-dependent. For example, the time-dependent rate for megathrust events on the Japan trench is lower than the long-term average, because Tohoku happened recently (compared to mean recurrence of about 500 yr). On the other hand, Nankai megathrust events happen on average every 100-150 years and the last event(s) was the 1944-1946 Nankai-Tonankai pair (more than half of the mean recurrence time has elapsed). The time-dependent rate is therefore higher than the long-term average (and also higher than the time-dependent rate on the Japan Trench).

A typical Monte Carlo simulation of equally probable time series, or periods presents a practical problem when modeling very long recurrence events (rare multi-fault or multi-segment ruptures in particular) as well as frequent smaller events: it requires a lot of realizations to represent the low rate events, and would sample the smaller events many more times than necessary to capture the variability of their impact on portfolio losses. In order to efficiently model all events, RMS developed a novel method to create timeseries of weighted periods. In this model, the weights assigned to each period span seven orders of magnitude, from 10^{-12} to 10^{-05}. This ensures that events whose rates span many orders of magnitude may be sampled in the same period (as they would in real catalogs). (see [4], for a more detailed description of the source model and simulation methodology)

When clients run their portfolios against this event set, they get a period loss table. It is a list of periods (each with a weight) that contain the losses coming from those events that were sampled in those periods. Whether the period is 1 year or covers a longer duration of insurance contract, one can extract from this table the average annual loss on that portfolio. This is also called Pure Premium or Technical Premium, because it is on average how much the insurance needs to get from the client to be even, in the long run. Other useful metrics have to do with reserve setting or risk transfer, and concern longer return periods of losses. However, there is another type of use of risk models, and it is defining an underwriting guideline that preserves enough diversification of risk. In other words, it is okay to take on more risks if they are not likely to take loss (often) from the same events.

To assess this, a useful quantity is expected loss correlation between two portfolios. If those portfolios correspond to different geographical regions, they can be viewed as a spatial correlation of losses.

Loss correlation coefficients, $\rho(CW_1, CW_2)$, are computed for pairs of geographic regions, City/Ward 1 and City/Ward 2, in Japan according to the equation in Fig. 4 below. The loss correlations are computed for the average annual loss (AAL) of the City/Wards.

The correlation coefficient represents the correlation of losses within the same simulated periods. Values range from -1 to 1, with 1 being fully correlated. We have used modeled period lengths of one year, therefore this study investigates correlation of annual insured losses. The weights of each period in this time series are accounted for in the correlation function by scaling the annual losses, $AL_n(CW_i)$, by the weight w_n associated with period *n*.

$$\rho(CW_1, CW_2) = \frac{\sum_{n=1}^{N}(w_n * AL_n(CW_1) * AL_n(CW_2)) - AAL(CW_1) * AAL(CW_2)}{STDDEV_{AL(CW_1)} * STDDEV_{AL(CW_2)}}$$

Where:

N is the number of periods in the simulated event set,

w_n is the weight of period *n*,

$AL_n(CW_i)$ is the annual loss for City/Ward *i* and period *n*,

$AAL(CW_i) = \sum_{n=1}^{N}(w_n * AL_n(CW_i))$ is the Average Annual Loss for City/Ward *i*, and

$STDDEV_{AL(CW_i)} = \sqrt{\sum_{n=1}^{N}(w_n * AL_n^2(CW_i)) - AAL^2(CW_i)}$ is the standard deviation of annual loss for City/Ward *i*.

Fig. 4 – Spatial correlation coefficient for regions CW_1 and CW_2.

Notably, the correlation coefficient is independent of absolute exposure value and absolute loss amount for each region. This means that two regions, with high and low AAL respectively, can have a large correlation coefficient if their annual losses behave similarly between simulation periods, particularly in strongly weighted periods. The converse, pairs with similar AAL but low correlation coefficient, is also possible.

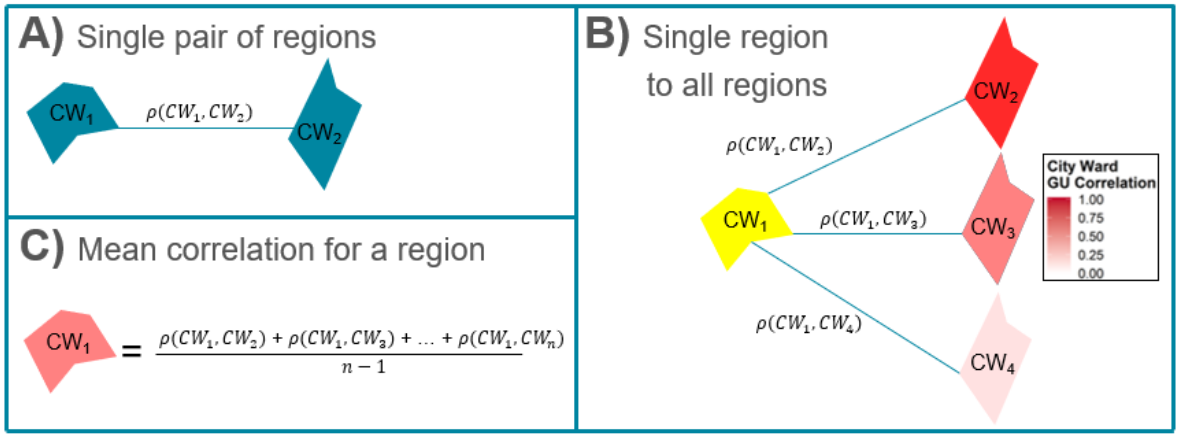

Fig. 5 – Graphical representations of three implementations of the correlation coefficient, ρ, as defined in Fig 4. A) Correlation coefficient between a single pair of regions. B) A single region to many regions. Example regions CW1, CW2, and CW3 are colored by their high, medium, and low correlation coefficients relative to

the base region in yellow. $\rho(CW_1, CW_1) = 1$. C) Mean of a base region to each other region. $\rho(CW_1, CW_2)$ is analogous to $\rho(CW_1, CW_2)$ in B.

Spatial loss correlations can be explored in a few ways using the correlation coefficient, the simplest of which is the correlation of two distinct regions, $\rho(CW_1, CW_2)$. This is displayed graphically in Fig. 5A. This metric enables us to understand the spatial trends of correlations when displayed as the correlation of a single region to all other defined regions as in Fig. 5B. This is accomplished by defining a base city ward for comparison to all other regions. These base regions will be displayed in yellow, and all others are displayed with a color representing their correlation coefficient with the base region as shown in Fig. 5B. The correlation of a region to itself, $\rho(CW_i, CW_i)$, is by definition equal to 1.

In order to evaluate how correlated a region is in general with all other regions, maps of mean correlation are generated as shown in Fig. 5C. The mean correlation for a region is the mean of all the correlations between it and the other regions. This metric is not normalized by distance. Two regions close to each other are more likely to experience similar hazard. The correlation of each other region to the base city ward equally influences the mean correlation metric, therefore base regions with many regions in close proximity tend to have higher mean correlations. In particular, this occurs in high population density cities/wards because they tend to have smaller areas and be closely grouped with other small highly populated cities/wards.

3. Results

3.1 Losses from Tsunami and Shake:

We present results based on Annual Average Losses (AAL) for the ground shaking and tsunami for coastal cities /city wards along the entire coast of Japan resulting from the RMS high-definition Japan earthquake and tsunami model. We used RMS Japan Earthquake Industry Exposure Database (IED) 2018 to identify the values of buildings and infrastructures in various lines of business including residential, industrial and commercial exposure. The AAL losses presented here, are measured at the city ward scale. In addition, we present AAL normalized by Total Insured Value (TIV) of each cityward, referred to as loss cost (LC). (Loss cost = AAL / TIV*1000).

The relative loss contributions of tsunami and shaking depend on various factors. For shake loss, the location and area of the rupture plane, the distance of the rupture plane from the building sites, the soil types, and the height of the buildings are crucial factors. For tsunami loss, the direction of the tsunami waves, topography and bathymetry, the complexity of the coastline profile, the slip distribution on the rupture plane and its impact on coastal deformation (subsidence/uplift, Fig. 3) and the land cover and land use information are the important factors. Tsunami waves can have devastating impact on the low-elevation areas that are close to the coastline but as the land elevation and/or the distance from the coastlines increases, the tsunami inundation diminishes. Shaking damage tends to occur more frequently compared to tsunami damage and often has a more local impact, while tsunami damage is comparatively rare but potentially more devastating. Single tsunamis can impact much larger regions and more distant locations as tsunami waves propagate far distances while the damaging effects of seismic waves decay much faster in comparison. The damage footprints have different characters due to the influencing factors. We consider tsunamis generated for offshore earthquakes with MW≥7.5. In general, these earthquakes can cause significant shake losses, but often only limited tsunami loss as the initial seafloor deformation does not very large tsunami waves, however, the spread of where the damage is observed may strongly vary.

Fig. 6 illustrates the loss cost of coastal city wards both for shake and tsunami. For shake loss, only the tsunamigenic earthquake events are considered for an equal comparison. This limits the sources to offshore interface and intraplate earthquakes as well as outer rise events. We find that the loss cost is in generally larger for shake than for tsunami, as expected. The south-eastern Japan coastlines, which are vulnerable to the earthquake events generated from the Nankai trough, show the dominant losses both for shake and tsunami.

However, the loss patterns are different for shake and tsunami. Coastal cities close to the ocean get high tsunami losses while tsunami losses drop drastically further inland. The coastal configurations play an important role on the tsunami losses. The impact of coastline configurations and possible coastal processes such as wave reflection and refraction can only be modeled using a detailed numerical solution.

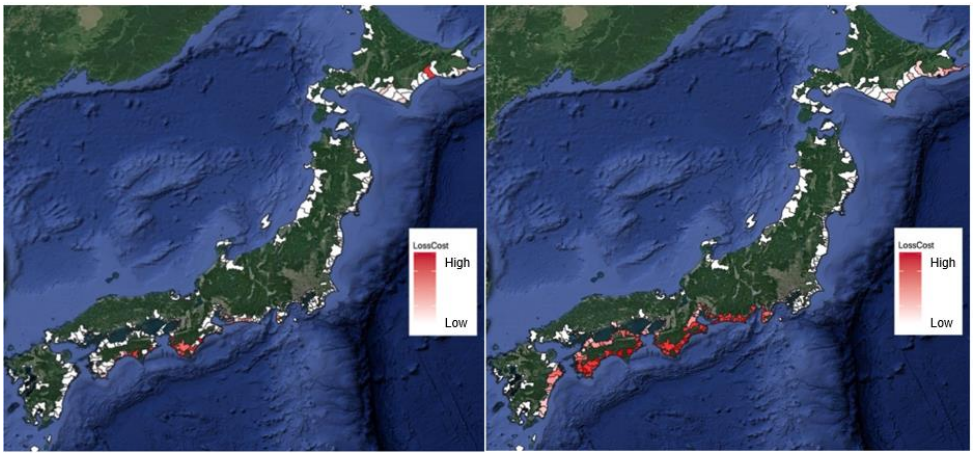

Fig. 6 – City ward loss cost (AAL / TIV*1000) for tsunami (left) and shake (right) for tsunamigenic earthquake events. The color scale is the same for each.

Fig. 7 presents the Average Annual Loss (AAL) for tsunami and shake hazards as well as the ratio of tsunami TS AAL (AAL only caused by tsunamis) over shake SH AAL (AAL only caused by shaking) for the coastal city wards. For both tsunami and shake, the maximum AALs are on the south-eastern coastline, however the ratio of TS AAL to SH AAL is highest at the north-eastern coastlines (Fig. 7, bottom). North-east of Japan is mostly vulnerable to the offshore Japan trench ruptures. Shake damages induced from the Japan trench along the northern side of Japan are small relative to those caused by Nankai sources in the south as the distances between exposure and the rupture planes are larger. Tsunami waves can travel further distances than seismic waves, so they produce larger AALs than shaking when the sources are further from the coast. Goda et al. (2018,[10]) saw similar results as they reported higher shake loss relative to tsunami loss for shorter return periods but higher tsunami loss relative to shake loss for longer return periods at Iwanuma, Ishinomaki, Onagawa, and Shizugawa cities. Along the south-eastern coastline, shake AAL is mostly greater than the tsunami AAL with the exceptions of Kainan, Goba, and Inami, Wakayama prefectures.

3.2 Spatial Correlations

For the remainder of this paper, when referencing shake losses, unless it is otherwise written, we are referring to the shake losses that are caused from the tsunamigenic events, i.e. events that also cause tsunami losses in our model. This choice leads to a useful comparison between tsunami and shake losses, otherwise shake losses would be influenced e.g. by crustal fault events that do not trigger a tsunami.

Maps of mean shake correlation, Fig. 8 left (detailed in the methodology, Fig. 5C), show two distinct patterns of correlations, the high consistent correlations in the southern City/Wards and the lower consistent correlations in the northern City/Wards. These higher mean correlations in the south are driven by Nankai sources. This is partly driven by the size and distance between city/wards. It is important to note that since this is a mean correlation value, it will be impacted by how geographically dense the city/wards are.

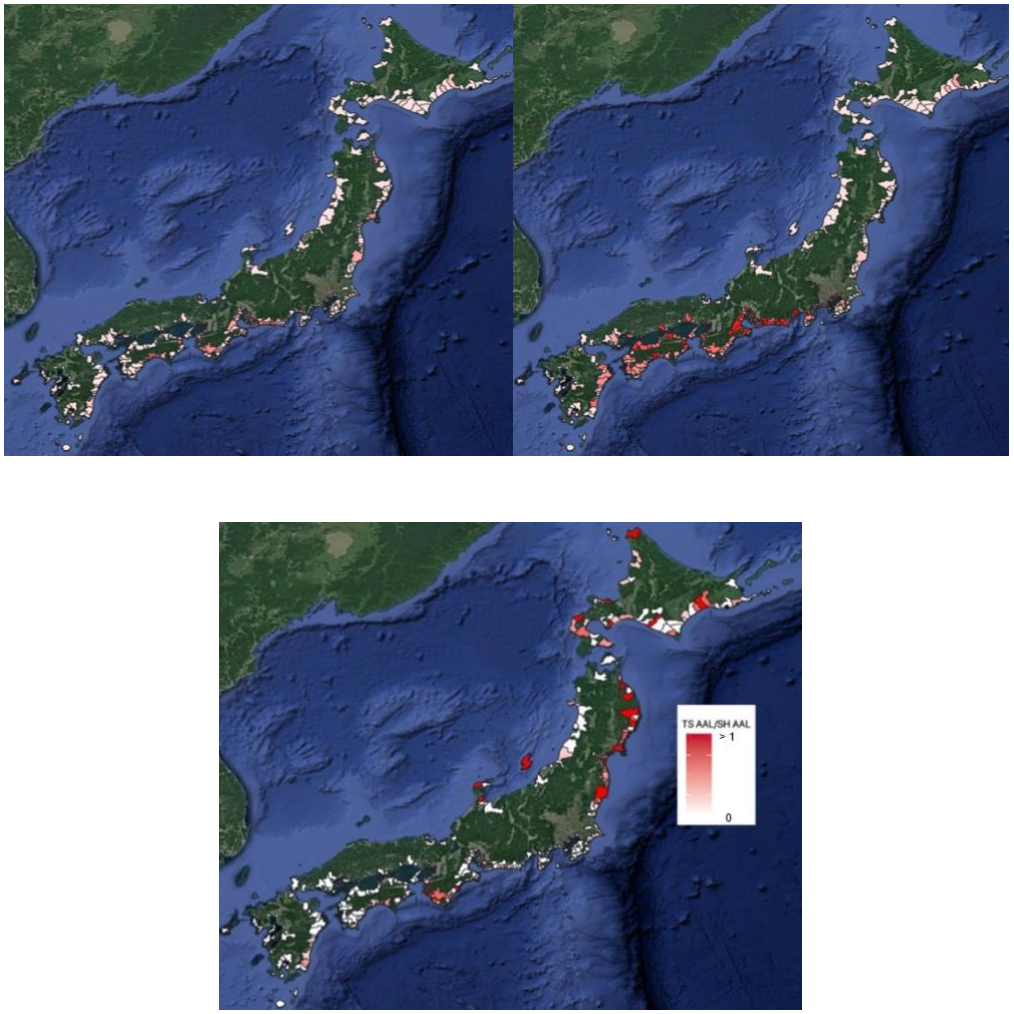

Fig. 7 –Tsunami AAL (top left) and shake AAL (top right) for the coastal city wards. The colors show highest AAL as red and lowest AAL as white. (bottom) Ratio of tsunami AAL to shake AAL. Only tsunamigenic events are considered.

The overall level of correlation in the northeastern coast is lower than that of the southern coast, for both shake and tsunami. In addition, shake and tsunami are very consistent with each other in the north. However, the tsunami correlations (Fig. 8, right) are very heterogeneous in the south. Within the heterogeneous pattern found in the south, there are some relatively high correlations (notice the difference in color scale between shake and tsunami) peaking in some of the most tightly populated bays but other similar exposure, such as Tokyo, does not show very much correlation. This stark contrast between the shake and tsunami correlation patterns on the complicated Southern coastline suggests that correlation of tsunami loss behave in a dramatically different fashion in that region, therefore shake correlations are an inadequate predictor of tsunami correlations there.

Focusing in on some of the higher loss city wards we can look at how they correlate with the rest of the nation. Tanabe-shi in Wakayama has a high loss for both tsunami and shake with about 50% of the AAL coming from either peril. The correlation by event description shows that the highest correlating CWs are driven by the Nankai losses, but unlike shake, this CW also correlates with the northern part of Japan for the Large Japan Trench events. The reason is that tsunami waves can have ocean-wide propagation and impact far regions.

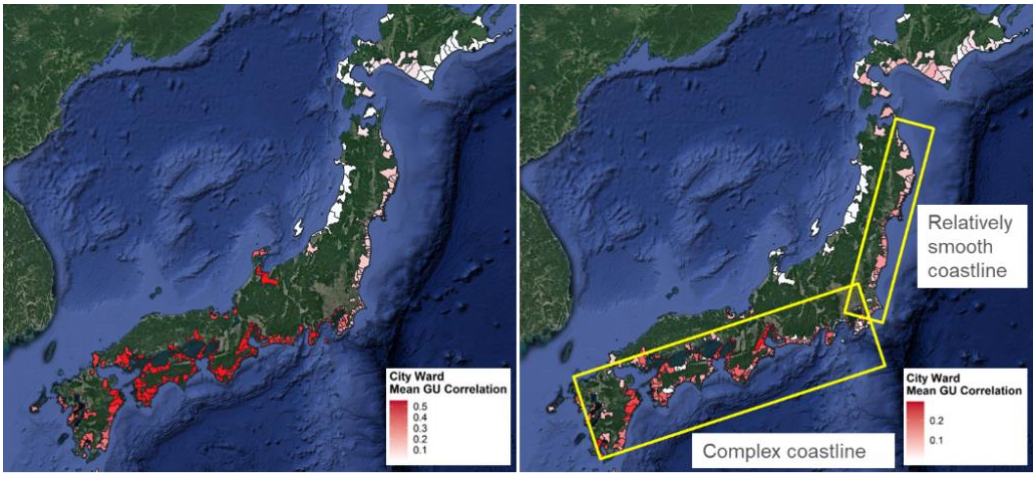

Fig. 8 – Mean correlations for shake (left) and tsunami (right). Yellow rectangles indicate different levels of complexity of the coastal geometry that influence tsunami correlation values. See Fig. 5C for more info about generating these figures.

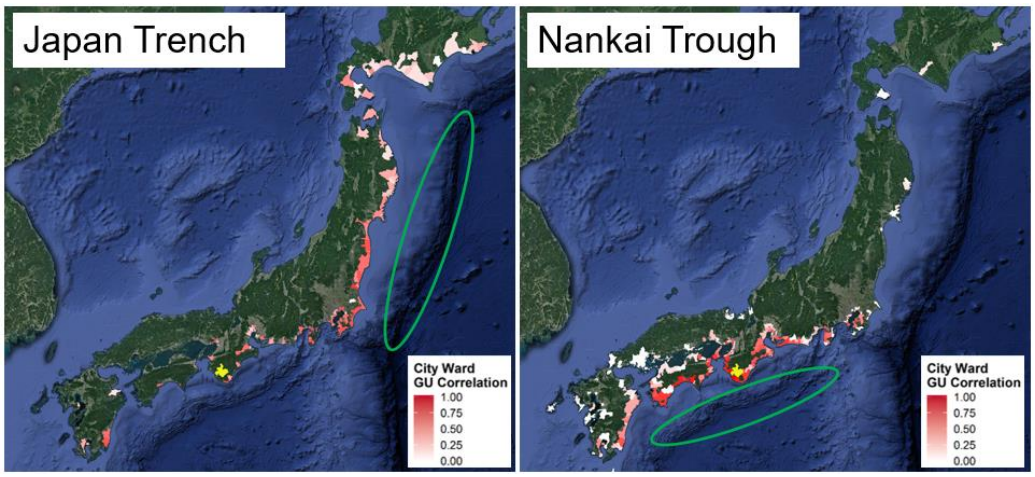

Fig. 9 – Tsunami loss correlation for the base city ward, Tanabe-shi (Wakayama prefecture), in yellow. Losses are subset to tsunami events from the specified source type, Japan Trench on the left and Nankai Trough on the right. The general source regions are highlighted in green. See Fig. 2 for more detailed source geometries.

4. Discussion

Both shake and tsunami are well-known risks in Japan. Even so, the 2011 Tohoku event was an unexpected catastrophe that deeply affected the people and the economy, in Japan and beyond. Since then, risk and hazard models worldwide have strived to incorporate all events that could not be ruled out, leading to the introduction of very large events in many countries. In Japan, those are in particular on subduction interfaces, like Nankai, Sagami, the Japan trench, and the Kuril trench. Our contribution concentrates on all events, M7.5 to M9+, that can produce both shake and tsunami losses in Japan. We use the RMS HD Japan Earthquake and Tsunami Risk Model to compare and contrast loss metrics patterns between the two causes of loss. The shake model is based on a detailed source model ([3], [4]) and a ground motion model that includes site amplification according to soil characteristics. The tsunami modeling starts from the earthquake sources and builds on them, with heterogeneous slip distributions, sea floor and coastline deformation, wave propagation and inundation model. The model is applied to the RMS Japan Industry Exposure Database 2018, at the city ward geocoding resolution.

We show both absolute and normalized average annual losses by city ward and correlations between city wards. The correlation metric allows to gain an understanding of the spatial differences in loss without the levels of exposure/absolute loss values driving the comparison.

Tsunami correlations are strongly influenced by the topography, bathymetry, coastline, slip distribution and deformation. For a relatively smooth coastline and where there is some distance between the source and the coast, like along the Japan Trench, the distance between city/wards is not impactful. In other words, the correlation is rather homogeneous along the coast since any seismic slip heterogeneity would be smoothed out by seismic wave propagation distance and the wave dynamics is not complicated by bays or other changes of orientation of the coast. On the contrary, the propagation of the tsunami waves through different coastline complexities can lead to differences in correlation for city/wards that are bordering each other. Such heterogeneity also happens where the coast is located close to the seismic slip patches. Both factors are impacting the city wards forming the southeast coast lines (in particular all around Shikoku and the coastlines facing it on the other islands).

The correlation level itself is also strongly influenced by the rate of the events. This is why the overall correlation level on the Japan trench is not very high: Tohoku just happened so the time-dependent rate of a M9 there is very low. On the contrary, the time-dependent chosen for large events on the Nankai trough can have an impact on loss correlation values along the coast (see Masuda et al for a quick review of published alternative models).

There are limits to this study. First, roughly 750 tsunami sources are used. Ideally, more tsunami realizations of each shake event would be simulated to provide a more complete picture of the possible variability in loss. The limiting factor mainly arises from the computational demand and access to sufficient computational resources to numerically solve the shallow water wave equation and determine inundation depths at a high resolution for many sources across the entire Japanese coastline. Second, projects aimed at better constraining the geometry of the seismic sources, the convergence rate, the coupling coefficient, the dating of past events through terrace uplift or paleo-tsunami studies are as essential to the quality of spatial loss correlation estimates as a high resolution near-coast bathymetry and a good integration of bathymetry and topography. Our results underline that detailed simulation-based probabilistic tsunami models are paramount to make informed decisions and that even limited versions can already provide guidance. Note that if the regions corresponding to the portfolios are heterogeneous in size, the interpretation of the mean correlation values needs to be done with care. While this study was meant to be exploratory, tsunami is a very high gradient peril and higher spatial resolution analyses are preferred [9].

In summary, our modelling results show that shake loss correlation values do not seem to be a good indicator for tsunami loss correlation values due to the very different nature of the loss causing process. We have shown strong variability in the shake and tsunami losses and their corresponding correlation patterns. This implies that tsunami losses may happen where shake losses were not expected (due to wave dynamics), and that different locations may be correlated for shake than for tsunami. This has a direct impact on the actual diversification of a portfolio. This is an essential conclusion as it is not an uncommon practice in the insurance industry to apply simple factors to shake losses to represent tsunami losses. The less diversified a portfolio, the larger the reserves, or the more risk transfer is needed. A good understanding of the spatial correlation of losses can help make business decisions and develop underwriting guidelines, ultimately leading to a more resilient society.

5. Copyrights

6.References

[1] Fitzenz DD, Taylor J, Spillers C (2018): Source model contributions to the spatial correlation of losses in earthquake risk models, *11th NCEE proceedings*.

[2] Fitzenz DD (2018): Conditional Probability of What? Example of the Nankai Interface in Japan, *BSSA* DOI:10.1785/012018001.

[3] Earthquake Research Committee, National Map of Earthquake Prediction Map 2016, President of the Earthquake Investigation Committee, 2016.

[4] Masuda M, William C, Sakai J, Fitzenz D, Seyhan E, Ancheta T, Farahani RJ, Woessner J, Dollarhide E (2020): A comprehensive probabilistic earthquake and tsunami risk model for Japan, *Conference Proceedings of the 17th WCEE*, Sendai, Japan.

[5] Farahani RJ, Woessner J, Bingi S, Masuda M (2020): Probabilistic tsunami hazard assessment along the entire Japan coastline, *Conference Proceedings of the 17th WCEE*, Sendai, Japan.

[6] Woessner J, Farahani RJ (2020) Tsunami inundation hazard across Japan, *International Journal of Risk Reduction*, under review.

[7] Melgar D, LeVeque RJ, et al. (2016): Kinematic rupture scenarios and synthetic displacement data: An example application to the Cascadia subduction zone, *Journal of Geophysical Research: Solid Earth*, https://doi.org/10.1002/2016JB013314.

[8] Kwak DY, Seyhan E (2020): Two-Stage Nonlinear Site Amplification Modeling for Japan with VS30 and Fundamental Frequency Dependency, *Earthquake Spectra* (in press)

[9] Goda K, Yasuda T, et al. (2017): Tsunami simulations of mega-thrust earthquakes in the Nankai–Tonankai Trough (Japan) based on stochastic rupture scenarios. *Geological Society, London, Special Publications*, SP456.1. https://doi.org/10.1144/SP456.1

[10] Goda K, Risi R D (2018): Multi-hazard loss estimation for shaking and tsunami using stochastic rupture sources, International Journal of Disaster Risk Reduction, **28**, 539-554.

